Uncovering a New Cause of Obstructive Hydrocephalus Following Subarachnoid Hemorrhage: Choroidal Artery Vasospasm–Related Ependymal Cell Degeneration and Aqueductal Stenosis–First Experimental Study

Coskun Yolas[1], Nuriye Guzin Ozdemir[2], Ayhan Kanat[3], Mehmet Dumlu Aydin[4], Papatya Keles[5], Umit Kepoglu[7], Nazan Aydin[8], Cemal Gundogdu[6]

BACKGROUND: **Hydrocephalus is a serious complication of subarachnoid hemorrhage (SAH). Obstruction of the cerebral aqueduct may cause hydrocephalus after SAH. Although various etiologic theories have been put forward, choroidal artery vasospasm–related ependymal desquamation and subependymal basal membrane rupture as mechanisms of aqueductal stenosis have not been suggested in the literature.**

METHODS: **This study was conducted on 26 hybrid rabbits. Five rabbits were placed in a control group, 5 were placed in a sham group, and the remaining rabbits ($n = 16$) were placed in the SAH group. In the first 2 weeks, 5 animals in the SAH group died. The other 21 animals were decapitated after the 4-week follow-up period. Choroidal artery changes resulting from vasospasm, aqueduct volume, ependymal cell density, and Evans index values of brain ventricles were obtained and compared statistically.**

RESULTS: **Mean aqueduct volume was 1.137 $mm^3 \pm 0.096$, normal ependymal cell density was 4560/$mm^2 \pm 745$, and Evans index was 0.32 ± 0.05 in control animals ($n = 5$); these values were 1.247 $mm^3 \pm 0.112$, 3568/$mm^2 \pm 612$, and 0.34 ± 0.15 in sham animals ($n = 5$); 1.676 $mm^3 \pm 0.123$, 2923/$mm^2 \pm 591$, and 0.43 ± 0.09 in animals without aqueductal stenosis ($n = 5$); and 0.650 $mm^3 \pm 0.011$, 1234/$mm^2 \pm 498$, and 0.60 ± 0.18 in animals with severe aqueductal stenosis ($n = 6$). The choroidal vasospasm index values were 1.160 ± 0.040 in the control group, 1.150 ± 0.175 in the sham group, 1.760 ± 0.125 in the nonstenotic group, and 2.262 ± 0.160 in the stenotic group. Aqueduct volumes, ependymal cell densities, Evans index, and choroidal artery vasospasm index values were statistically significantly different between groups ($P < 0.05$).**

CONCLUSIONS: **Ependymal cell desquamation and subependymal basal membrane destruction related to choroidal artery vasospasm may lead to aqueductal stenosis and hydrocephalus after SAH.**

INTRODUCTION

Despite the increased use of technology in neurosurgical practice,[1,2] spontaneous subarachnoid hemorrhage (SAH) still leads to significant morbidity and mortality.[3-5] Acutehydrocephalus is a common life-threatening complication after SAH and has seldom been studied in animal models.[6] The frequency of hydrocephalus after SAH ranges from 15% to 20%, and it is an important prognostic factor.[7] Impaired cerebrospinal fluid (CSF) flow and decreased absorption secondary to fibrosis of the leptomeninges and arachnoid granulations as a result of blood product deposition were accepted as causes of hydrocephalus after SAH. In addition, the inflammatory process is an important factor in the pathophysiology of hydrocephalus, and there is increased interest in the investigation of changes involving the inflammatory processes that occur after SAH.[8] Inflammation of the meninges or ventricles secondary to infection or hemorrhage leads to hydrocephalus through the

Key words
- Aqueductal stenosis
- Choroidal artery vasospasm
- Ependymal cell desquamation
- Hydrocephalus
- Subarachnoid hemorrhage

Abbreviations and Acronyms
CP: Choroid plexus
CSF: Cerebrospinal fluid
EI: Evans index
SAH: Subarachnoid hemorrhage

From the [1]Erzurum Training and Research Hospital, Neurosurgery Clinic, Erzurum; [2]Istanbul Training and Research Hospital Clinic, Istanbul; [3]Department of Neurosurgery, Recep Tayyip Erdoğan University Faculty of Medicine, Rize; Departments of [4]Neurosurgery, [5]Anatomy, and [6]Pathology, Ataturk University Faculty of Medicine, Erzurum; [7]Department of Neurosurgery, Bahcesehir University Faculty of Medicine, Istanbul; and [8]Psychiatry Clinic, Bakırkoy Training and Research Hospital for Psychiatry, Neurology and Neurosurgery, Istanbul, Turkey

To whom correspondence should be addressed: Ayhan Kanat, M.D.; Mehmet Dumlu Aydin, M.D. [E-mail: ayhankanat@yahoo.com; nmda11@hotmail.com]

Citation: World Neurosurg. (2016) 90:484-491.
http://dx.doi.org/10.1016/j.wneu.2016.03.049

Journal homepage: www.WORLDNEUROSURGERY.org

Available online: www.sciencedirect.com

impairment of CSF circulation and absorption or the normal dampening of arterial pulsations. Ventriculitis can induce ependymal scarring, intraventricular obstruction, and multicompartment hydrocephalus.[9] Parasympathetic dysfunction may also play a role in triggering both the vasospasm and the inflammation process, beginning with desquamation and basal membrane rupture.[10] All these mechanisms can lead to third ventricle or aqueduct occlusion. Understanding of the pathology after SAH continues to evolve. Pathology in the periaqueductal region after SAH seems to be important. However, the relationship of choroidal artery vasospasm to ependymal desquamation of the aqueduct and basal membrane rupture to our knowledge has never been studied. Aqueductal stenosis may be the key problem in hydrocephalus after SAH. We studied choroidal artery vasospasm–related aqueductal stenosis, and we present here a new model explaining the pathophysiology of hydrocephalus.

MATERIALS AND METHODS

This study was performed according to animal protocols approved by the Ethics Committee of Ataturk University, Medical Faculty. The care of the animals and the experiment were conducted according to the guidelines set forth by the ethics committee.

Experiment

This study was conducted on 26 hybrid rabbits (2.5 years old, 4.2 kg ± 0.6); 5 rabbits were placed in a control group, 5 were placed in a sham group, and the remaining 16 rabbits were placed in the SAH group. A balanced, injectable anesthetic was used to reduce pain and mortality. After anesthesia was induced with isoflurane given by a face mask, 0.2 mL/kg of the anesthetic combination (ketamine 150 mg/1.5 mL, xylazine 30 mg/1.5 mL, and distilled water 1 mL) was subcutaneously injected before surgery. During the procedure, a dose of 0.1 mL/kg of the anesthetic combination was used when required. Autologous blood (1 mL) was taken from the auricular arteries and injected using a 22-gauge needle into fourth ventricle of animals in the SAH group over the course of 1 minute. After blood injection and formation of SAH, 5 animals died. The remaining 11 animals were included in the study. In the sham group, 1 mL of serum saline was injected into the cisterna magna. The animals in the control group were not subjected to this procedure. The animals were followed for 4 weeks without any medical treatment and then sacrificed. Whole bodies of all animals were kept in 10% formalin solutions after required cleaning procedures for retrograde histologic examination.

Histopathologic Procedures

To estimate the ependymal cell density of the ventricular surfaces of aqueducts, Evans index (EI), and aqueduct volumes, all brains were sectioned coronally at the levels of the most enlarged parts of brains at the levels of biparietal parietal coni. For aqueduct volume and ependymal cell estimation, longitudinal brainstem sections were performed at the brainstem levels. The brain sections were horizontally embedded in paraffin blocks to observe all the ventricles and aqueducts during the histopathologic examination. Consecutive sections of 5 μm were acquired ($n = 20–50$ for each brain). The sections were stained with hematoxylin-eosin, Masson's Trichrome, and terminal deoxynucleotidyl transferase [TdT] dUTP nick-end labeling (tunel) stains. Stereologic analyses of histopathologic data were done according to principles described previously.[11-13] The Cavalieri method was used to evaluate the density of ependymal cells in the aqueductal spaces and the volumes of aqueducts. Figure 1A shows a macroscopic view of an animal after SAH. Histopathologic appearances of aqueductal surfaces, choroid plexuses (CPs) and ventricles are seen in Figure 1B. Many consecutive sections were obtained from tissue samples from one side to the other side of aqueducts and then arranged over and over, and imaginary aqueducts were created as cylinders. The volumes of all aqueducts were calculated using cylinder methods with the following formula: $V = \pi r^2 h$ (Figure 2). To estimate the EI, photographs were taken on prepared forms of glass lamellae, and bifrontal cornual indexes were calculated using minisquared papers (Figure 2). Ependymal cell density was estimated as cell numbers/mm² of aqueductal surfaces transferred into cylindrical shapes, and ependymal cells accepted as curbs as shown in Figure 3A and B. The height of the model cylinder was 50 μm, and the radius was estimated as 25 μm by using a microscopic scale bar (Figure 3A). The surface values of our model cylinder were calculated using the formula 2μrh. The mean cell values were documented as cell numbers/mm², and this value was calculated as 3.925 μm². Because each ependymal length was estimated as 6 μm, we estimated that the cylindrical height of our model was equal to 8.5 ependymal cell height, and the bottom circle was equal to (2μr/6 = 150/8): 18.75 ependymal cells long (Figure 3C). Each model cylinder included 18.75 × 8.5 = 159.375 ependymal cells. Choroidal artery vasospasms were assessed as described Yılmaz et al.[14] According to the method of Yılmaz et al.,[14] luminal diameters of anterior

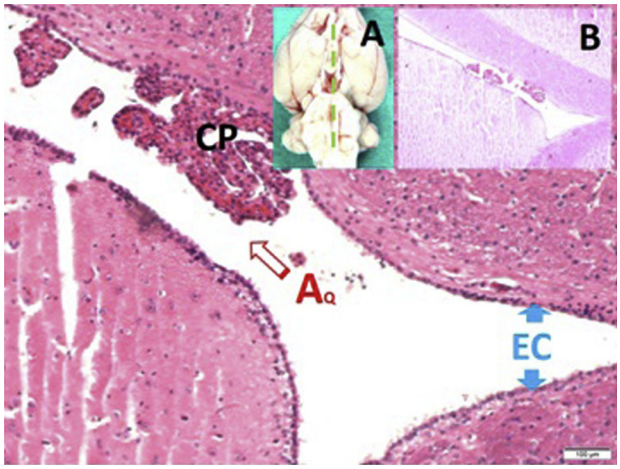

Figure 1. In a rabbit with subarachnoid hemorrhage, normal brain (**A**) and normal aqueduct (A_Q). (**B**) Histologic appearance (light microscopy, hematoxylin-eosin, ×4). Histologic appearance of choroid plexus (CP) and ependymal cells (EC) in high magnification (light microscopy, hematoxylin-eosin, ×10).

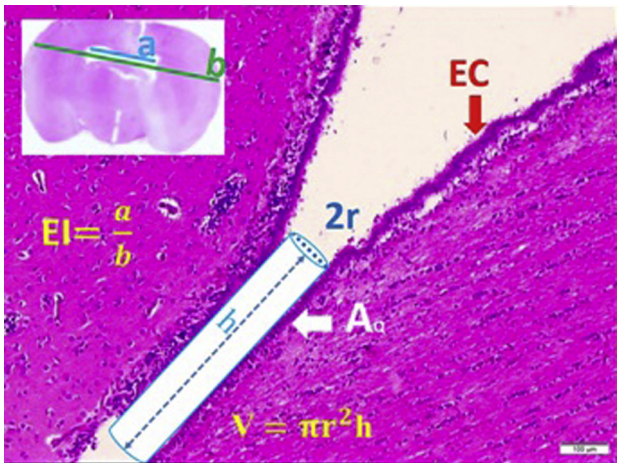

Figure 2. In an animal from the control group, normal brain ventricles, ependymal cells (EC), and aqueduct (Aq) (light microscopy, hematoxylin-eosin, ×4). Evans index and aqueductal volume formulas are shown at the left and bottom.

choroidal artery branches just entering into choroid plexus were examined and measured using the micrometric microscopic scale bar. The mean volume values of all bilateral ChA were calculated using the following formula: $V = \pi r^2 h$. The choroidal artery vasospasm index was calculated using the following formula: VSI = $(R^2 - r^2)/r^2$ (VSI = choroidal artery vasospasm index, R = choroidal artery external radius, r = choroidal artery internal radius). The choroidal artery vasospasm index was 1–1.5 in animals with no vasospasm; 1.5–2 in animals with slight vasospasm; and >2 in animals with severe vasospasm.

The data were analyzed using SPSS for Windows 12.0 (SPSS, Inc., Chicago, Illinois, USA). The data analysis consisted of the Kruskal-Wallis and Mann-Whitney U tests. Differences were considered to be significant at $P < 0.05$.

RESULTS

In this experimental model of SAH, the brains of 11 (which survived up to 4 weeks) of 16 rabbits with SAH, 5 sham-SAH animals, and 5 naïve animals as controls (n = 21 animals) were analyzed. Massive subarachnoid fourth ventricular hemorrhage was observed in animals of the SAH groups. They showed meningeal irritation signs. Brain edema, stiffness, leptomeningeal thickness, and increased brain weight were seen in all animals that developed SAH. In 2 animals, cerebellar laceration was also detected. On histopathologic examination, ventricular surfaces, CP swelling, blood cell collection in the CP sulci without adhesion or thrombus formation, ependymal cell edema, desquamation, and basal membrane ruptures were seen (Figures 4 and 5). Apoptosis, ependymal desquamation, and subependymal thrombus formation were detected to some extent with terminal deoxynucleotidyl transferase [TdT] dUTP nick-end labeling stain (Figure 6). In animals that developed massive hydrocephalus (n = 6), ependymal cell loss, subependymal basal membrane rupture, and necrotic ventricular materials were observed in aqueductal channels (Figure 6). In some animals, pan intra-aqueductal ependymal cell desquamation, basal membrane rupture, and clot formation were observed (Figures 4–6). Choroidal artery vasospasm–related basal membrane rupture, ischemia, and clot

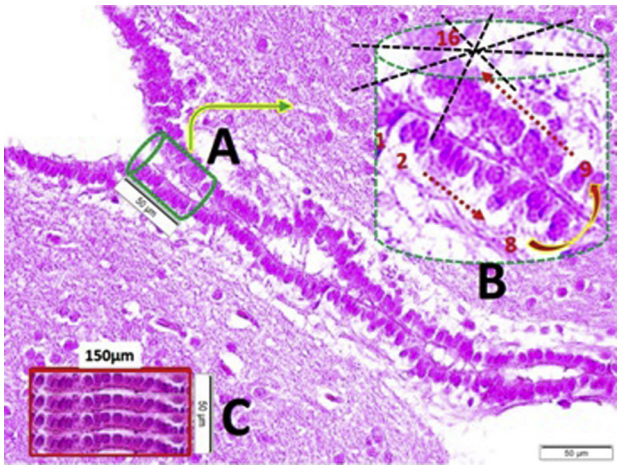

Figure 3. (**A**) Ependymal cell density was estimated as cell numbers/mm^2 of aqueductal surfaces, which are depicted as cylindrical shapes with ependymal cells depicted as kerbs. (**B**) The height of the model cylinder was 50 μm, and the radius was estimated as 25 μm by using a microscopic scale bar. The surface values of our model cylinder were calculated using the following formula: 2μrh. The mean cell values were documented as cell numbers/mm^2, and this value was calculated as 3.925 μm^2. (**C**) Each ependymal length was estimated as 6 μm, the height of our model cylindrical height is equal to 8.5 ependymal cell height, and the bottom circle is equal to (2μr/6 = 150/8): 18.75 ependymal cells long. Each model cylinder included 18.75 × 8.5 = 159.375 ependymal cells. This is equal to 4.560 ± 745/mm^2.

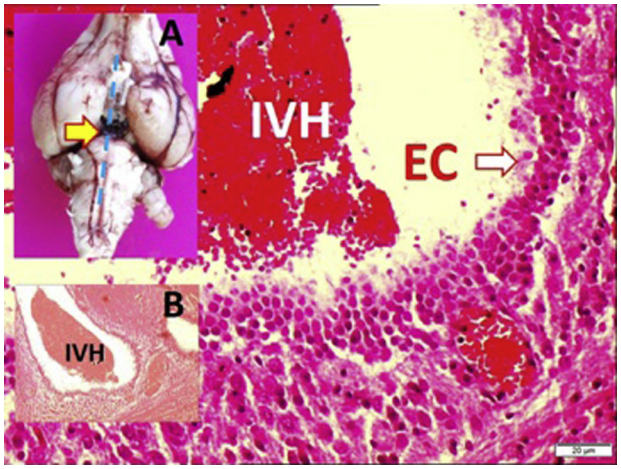

Figure 4. Normal ependymal cells without thrombus in high magnification (light microscopy, hematoxylin-eosin, ×20). (**A**) The brain of a rabbit at midsection level (*arrow*) to explore the aqueduct. (**B**) Bloody ventricles (intraventricular hemorrhage [IVH]) (light microscopy, hematoxylin-eosin, ×4).

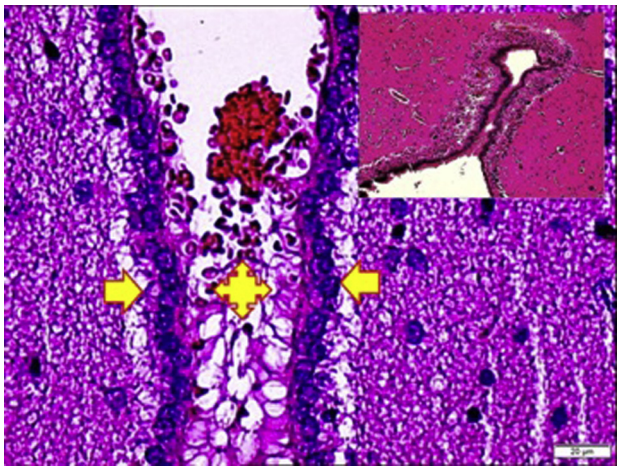

Figure 5. Ependymal cell reaction with separated basal ependymal lamina in high magnification (light microscopy, tunel stain, ×10). (Right top inset) Bloody aqueduct (light microscopy, tissue culture medium, ×4). Two arrows show rupture of the subependymal basal membrane; symbol with four arrows indicate ciliary process adhesivity.

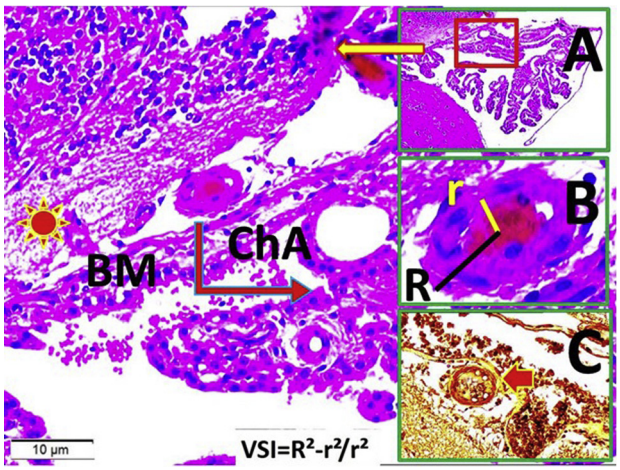

Figure 7. Choroidal artery (ChA) between the basal lamina (*yellow-red star*) and subependymal basal membrane (BM) (light microscopy, hematoxylin-eosin, ×10) is seen in a normal rabbit. (**A**) Choroid plexus (light microscopy, hematoxylin-eosin, ×4). (**B**) Vasospasm index formula in a normal rabbit (light microscopy, hematoxylin-eosin, ×20). (**C**) Apoptotic nonfunctional choroidal artery (*arrow*) and periarterial desquamated ependymal cell, blood cell, and atrophic choroid plexus cell accumulation over the gliotic periaqueductal surfaces in a rabbit with subarachnoid hemorrhage (light microscopy, terminal deoxynucleotidyl transferase [TdT] dUTP nick-end labeling, ×4).

formation and bleeding just under the degenerated-desquamated ependymal cells were noted (Figures 7–10). In hydrocephalic brains with greater EI (>0.5%), aqueductal stenosis was prominent. The mean radius (r) and height (h) values of the aqueduct were 350 μm ± 76 and 2.140 μm ± 210, respectively. The surface value of our model cylinder was calculated as 3.925 μm² (18.75 × 8.5 = 159.375 ependymal cells/mm²). Mean volume of aqueduct, normal ependymal cell density, and EI were 1.137 mm³ ± 0.096, 4560/mm² ± 745, and 0.32 ± 0.05 in control animals ($n = 5$); 1.247 mm³ ± 0.112, 3568/mm² ± 612, and 0.34 ± 0.15 in sham animals ($n = 5$); 1.676 mm³ ± 0.123, 2923/mm² ± 591, and 0.43 ± 0.09 in animals without aqueductal stenosis ($n = 5$); and 0.650 mm³ ±

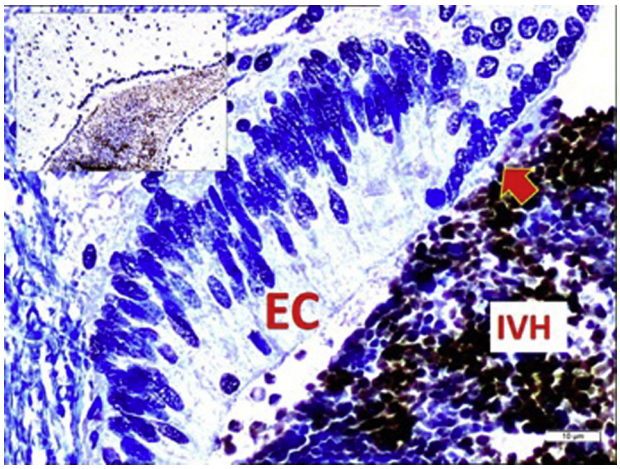

Figure 6. Ependymal cell reaction (EC) with some desquamated ependymal cells and separated basal ependymal lamina with thrombus (light microscopy, terminal deoxynucleotidyl transferase [TdT] dUTP nick-end labeling, ×10). (Left top inset) Bloody and thrombosed aqueduct (light microscopy, terminal deoxynucleotidyl transferase [TdT] dUTP nick-end labeling, ×4). IVH, intraventricular hemorrhage.

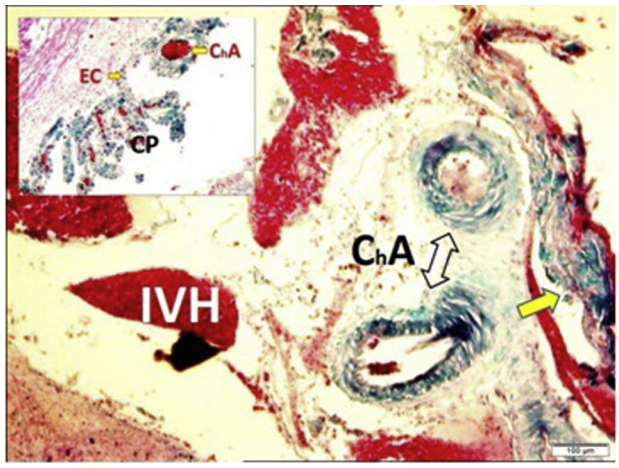

Figure 8. Spastic ChA and bleeding just under the degenerated-desquamated ependymal cells (*arrow*) within fresh bloody ventricles as a result of rupture and rebleeding of choroidal arteries (light microscopy, hematoxylin-eosin, ×10). (Left top inset) Normal choroidal artery (ChA), choroid plexus (CP), and ependymal cells (EC) (light microscopy, hematoxylin-eosin, ×4). IVH, intraventricular hemorrhage.

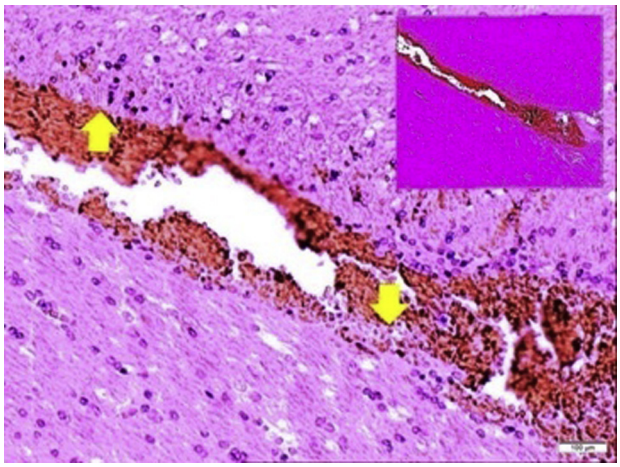

Figure 9. Accumulation of blood cells on ruptured basal membrane just under the desquamated ependymal cells (*arrows*) (light microscopy, hematoxylin-eosin, ×20). (Right top inset) Thrombosis development in aqueduct (light microscopy, hematoxylin-eosin, ×4).

0.011, 1234/mm² ± 498, and 0.60 ± 0.18 in animals with severe aqueductal stenosis ($n = 6$).

The choroidal artery vasospasm index values were 1.160 ± 0.040 in control group, 1.150 ± 0.175 in sham group, 1.760 ± 0.125 in nonstenotic group, and 2.262 ± 0.160 in stenotic group. According to choroidal artery vasospasm index values, the stenotic group was observed to have severe vasospasm (>2). The relationships between the aqueduct volume, ependymal cell density, EI, and choroidal artery vasospasm index values were meaningful statistically ($P < 0.05$) (Table 1).

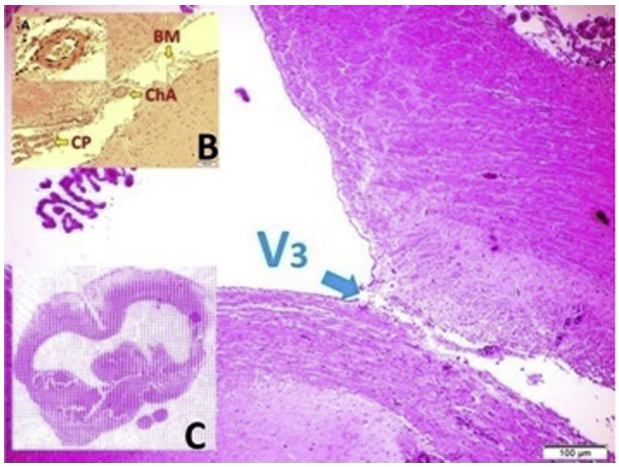

Figure 10. Development of aqueductal stenosis with enlarged third ventricle (light microscopy, hematoxylin-eosin, ×10). (**A**) High magnification shows choroidal artery just under the ependymal cells (light microscopy, hematoxylin-eosin, ×20). (**B**) Choroidal artery (ChA), choroid plexus (CP), and ruptured basal membrane (BM) (light microscopy, hematoxylin-eosin, ×4). (**C**) Prominent hydrocephalus (light microscopy, hematoxylin-eosin, ×4).

Table 1. Choroidal Artery Vasospasm Index, Mean Aqueduct Volume, Ependymal Cell Density, and Evans Index Values in Control, Sham, and Subarachnoid Hemorrhage (Nonstenotic and Stenotic) Groups ($P < 0.05$)

Parameter	Control Group	Sham Group	SAH Group	
			Nonstenotic	Stenotic
CVI	1.160 ± 0.040	1.150 ± 0.175	1.760 ± 0.125	2.262 ± 0.160
Mean aqueduct volume (mm^3)	1.137 ± 0.096	1.247 ± 0.112	1.676 ± 0.123	0.650 ± 0.011
Ependymal cell density ($/mm^2$)	4560 ± 745	3568 ± 612	2923 ± 591	1234 ± 498
EI	0.32 ± 0.05	0.34 ± 0.15	0.43 ± 0.09	0.60 ± 0.18

SAH, subarachnoid hemorrhage; CVI, choroidal artery vasospasm index; EI, Evans index.

DISCUSSION

Hydrocephalus is an important complication of SAH. A better understanding of the physiopathology of hydrocephalus may improve the outcome of patients with SAH.[15] For that reason, prevention and treatment of hydrocephalus after SAH are a major goal in neurosurgery. The ventricular system consists of 2 lateral ventricles connected to the third ventricle through the interventricular foramina. The third ventricle communicates with the fourth ventricle through the cerebral aqueduct. Having broad knowledge of anatomy is essential for practicing neurosurgery. Certain anatomic structures require detailed study because of their functional importance.[16-18] One of these structures is the cerebral aqueduct. Understanding the anatomy of the aqueduct is important to achieve good outcomes for patients with hydrocephalus after SAH. The aqueduct is relatively short and runs dorsally to end in the large cranial part of the fourth ventricle. The mean length of the aqueduct is 1–2 mm in rabbits.[19] The ependymal lining consists of 2 different cell types: normal ependymal cells and tanycytes connected to blood vessels or neuronal elements.[19] In histologic studies, tanycytes were found in the ependyma of the cerebral tissue of the cerebral aqueduct of neonatal and adult rabbits. Regarding the anatomy of this region, recent theories on the etiology of hydrocephalus have been suggested. The classic understanding of hydrocephalus, occurring as a result of obstruction to bulk flow of CSF, is evolving to models that incorporate dysfunctional cerebral pulsations and brain compliance.[7,17] Choroidal artery vasospasm–related ependymal desquamation of the aqueduct and basal membrane rupture have not been reported in the literature. In this study, we suggest that aqueductal stenosis is related to vasospasm of the choroidal artery and desquamation of the ependymal cells. In the acute stage of SAH, choroidal artery vasospasm results in periaqueductal hemorrhage. Parasympathetic

dysfunction may also play a role in triggering both the vasospasm and the inflammation process beginning with desquamation and basal membrane rupture.[10] The role of the petrosal ganglion of the glossopharyngeal nerve in vasospasm of the choroidal arteries was discussed in the literature.[17,20] The neuronal density of this ganglion cell seems to play an important role in the vesicle number of CP after SAH.[17,20] In both studies, the authors showed that the mean number of degenerated neuronal density of petrous ganglion was significantly different in the early and late decapitated groups.[17,20] A linear relationship was noted between the degenerated neuronal density in the petrous ganglion of the glossopharyngeal nerve and water-filled vesicle number of CP in the acute phase of SAH; however, an inverse relationship was observed in the late-chronic phase,[17,20] so degenerated neuronal density of the ganglion of glossopharyngeal nerve might be an important factor in the pathogenesis of hydrocephalus after SAH.[17,21] In the present study, we report for the first time aqueductal volume stenosis as a result of desquamation of the ependymal cells of the aqueductal region secondary to vasospasm of the choroidal artery. Choroidal artery vasospasm may be lead to reduced aqueductal volume and stenosis. Another cause of impaired CSF flow and decreased absorption may be fibrosis of the leptomeninges and arachnoid granulations as a result of blood product deposition. Also, partial obstruction of the fourth ventricular outflow and subsequent impaired CSF absorption may play a role.[22] Proving hypersecretion by vesicles as a cause of hydrocephalus would improve the outcome of patients.[23,24] Most available information about early brain injury after SAH comes from animal models of endovascular filament perforation.[25] The literature regarding hydrocephalus after SAH consists of human case series, most of which are retrospective. In retrospective human studies, it is impossible to clarify the exact pathogenic mechanism of hydrocephalus after SAH.[26,27] The morphologic mechanisms leading to the pathology remain elusive. For this reason, animal studies are welcome. Several criteria regarding the presence of acute and chronic hydrocephalus in rabbits, the relationship between increased CSF production and hydrocephalus in the absence of an obstruction after SAH, and the relationship of water vesicles and increased CSF production have been presented in the literature.[17,23] These studies suggest an important potential hypothesis of increased CSF production in the development of hydrocephalus after SAH.[17,23] It is likewise possible that CSF blockage per se leads to hydrocephalus, and the morphologic changes are sequelae that occur later in the disease course. These kinds of animal studies are important because it is difficult to evaluate these water vesicles of the CP in vivo or in human autopsy specimens for 2 reasons: first, these vesicles disappear 2 days after SAH; second, circulatory collapse after death may have some effect on the size and number of these water vesicles. In our study, we present findings supporting the new models highlighting the pathophysiology of hydrocephalus. Our findings suggest a new cause of aqueductal stenosis and hydrocephalus resulting from desquamation of ependymal cells secondary to choroidal artery vasospasm. In the present study, we histopathologically observed swelling of choroid plexus, ependymal cell edema, desquamation, ciliary droppings, and basal membrane ruptures (**Figures 6, 7**, and **9**). Choroidal artery vasospasm, ependymal cell loss, and subependymal basal membrane rupture in the aqueductal channel were related to the stenosis (**Figure 10**). Choroidal artery vasospasm led to basal membrane rupture. The separation of the cylindrical basal membrane of the aqueduct is followed by regeneration and reorganization. Fibrin tissue was observed to precipitate on basal membranes. Inert membrane-like fibrinolytic pathology was also noted. The ependymal cell desquamation led to necrosis, and they formed a plug with the blood products in the aqueduct. Finally, choroidal artery vasospasm led to endothelial microbleeding and basal membrane rupture resulting in gliosis and aqueductal stenosis, and mechanical obstruction occurred.

Our findings are valuable because the balance between cell proliferation and cell death is crucial in all tissues, particularly in the nervous system.[18] Hydrocephalus after SAH is accepted as an important prognostic factor.[7] Any contribution to knowledge of the cause of the morbidity and mortality of SAH is always welcome.[28] The main aim of the present study was to uncover the effect of choroidal artery vasospasm on aqueductal stenosis leading to hydrocephalus, which occured by ependymal desquamation and subependymal basal membrane rupture. In a subset of animals, aqueductal stenosis and supratentorial ventricular dilation occurred. We suggested that these changes developed secondary to vasospasm of the choroidal artery. However, aqueductal occlusion is not a sole cause of hydrocephalus after SAH because we also observed clot formation and hemorrhages. Also in our study, there was "rebleeding from choroidal arteries rupture" at 4 weeks after injection of blood (**Figure 8**), and mean aqueduct volume was reduced as a result of choroidal artery vasospasm—related low normal ependymal cell density in the aqueduct. We also assessed these parameters a short time after the injection to see their direct effects on the animals. In 2 animals, cerebellar laceration was also detected. On histopathologic examination, ventricular surfaces, CP swelling, blood cell collection in the CP sulci without adhesion or thrombus formation, ependymal cell edema, desquamation, and basal membrane ruptures were seen (**Figures 4** and **5**). What damage is initially caused simply by injection of blood in this extremely confined space? This question is difficult to answer. Cisternal blood injection has an acute effect on the brainstem and cranial nerve compression. CSF circulation problems and some nutritional problems of periventricular organs may occur. During cisternal blood injection, dural irritation may stimulate vasospasm and increased ICP. As shown in **Figures 5** and **6**, desquamated ependymal cells, ruptured basal membrane, and particles in the concentrated products in CSF adhere to each other and develop new membrane formations in the aqueduct, resulting in aqueductal stenosis.

Vasospasm of the choroidal arteries and subependymal basal membrane rupture caused the desquamation of the epithelial cells after SAH. The process resulted in adhesions and aqueductal volume reduction and stenosis. This is a novel finding that may have an important role in development of hydrocephalus after SAH. An evolving body of knowledge demonstrates that endovascular treatment of SAH may result in lower mortalities and morbidities,[28] and it has been suggested that coiling should be considered as a first-line treatment in aneurysmal SAH.[29] How can endovascular treatment of an aneurysm prevent aqueductal

stenosis with choroidal artery vasospasm? SAH clot removal, which can be accomplished only by conventional microsurgery, may be important in preventing aqueductal stenosis with choroidal artery vasospasm. It is imperative to understand this process to determine a better treatment option. In a human study, patients undergoing endovascular treatment more often received shunts compared with patients undergoing surgical aneurysm repair.[30] Although our study is experimental and involves a rabbit SAH model, it may have some relevance to human SAH. Our findings have great functional importance. We are the first to report aqueductal stenosis with choroidal artery vasospasm after SAH and that the recognition of this is important to prevent this complication. If one is the first to report something, that something is of value.[31-33] The opening of new horizons of this kind of knowledge will aid understanding of the complex challenge of hydrocephalus after SAH. More data are needed on this subject.

This study has some limitations. This is an experimental, observational study in a rabbit SAH model, and our experimental rabbit model of SAH may not accurately mimic the human disease process.[16,23,24,28] Perhaps the most important limitation of the study is that it is difficult to evaluate these changes in vivo or through autopsy, particularly in humans with SAH.[34] In this study, we propose that vasospasm of the choroidal artery is a major contributing factor of hydrocephalus after SAH. However, our results cannot be generalized with only 1 study, and further studies are needed.

CONCLUSIONS

Vasospasm of the choroidal arteries and desquamation of the ependymal cells are major factors leading to aqueductal volume reduction. Removing clots in the aqueductal region and preventing vasospasm of the choroidal artery may be important in preventing aqueductal stenosis and hydrocephalus after SAH. We present a preliminary experimental study to understand the mechanism of hydrocephalus after SAH. New studies aiming to address our findings may help increase understanding of this potential mechanism of hydrocephalus after SAH and develop a treatment in humans.

REFERENCES

1. Akca N, Ozdemir B, Kanat A, Batcik OE, Yazar U, Zorba OU. Describing a new syndrome in L5-S1 disc herniation: sexual and sphincter dysfunction without pain and muscle weakness. *J Craniovertebr Junction Spine*. 2014;5:146-150.

2. Kanat A, Yazar U, Ozdemir B, Coskun ZO, Erdivanli O. Frontal sinus asymmetry: is it an effect of cranial asymmetry? X-ray analysis of 469 normal adult human frontal sinus. *J Neurosci Rural Pract*. 2015;6:511-514.

3. Li J, Su L, Ma J, Kang P, Ma L, Ma L. Endovascular coiling versus microsurgical clipping for patients with ruptured very small intracranial aneurysms: management strategies and clinical outcomes of 162 cases. *World Neurosurg*. http://dx.doi.org/10.1016/j.wneu.2015.11.079 [Epub ahead of print].

4. Stranjalis G, Loufardaki M, Koutsarnakis C, Kalamatianos T. Trends in the management and hospital outcome of spontaneous subarachnoid hemorrhage in the post-international subarachnoid aneurysm trial era in Greece: Analysis of 719 patients during a 13-Year period. *World Neurosurg*. 2016;88:327-332.

5. Alotaibi NM, Nassiri F, Badhiwala JH, Witiw CD, Ibrahim GM, Macdonald RL, Lozano AM. The most cited works in aneurysmal subarachnoid hemorrhage: a bibliometric analysis of the 100 most cited articles. *World Neurosurg*. 2016;89:587-592.

6. Egashira Y, Xi G, Chaudhary N, Hua Y, Pandey AS. Acute brain injury after subarachnoid hemorrhage. *World Neurosurg*. 2015;84:22-25.

7. Shah AH, Komotar RJ. Pathophysiology of acute hydrocephalus after subarachnoid hemorrhage. *World Neurosurg*. 2013;80:304-306.

8. Welling LC, Welling MS, Teixeira MJ, Figueiredo EG. Neuroinflammation after subarachnoid hemorrhage: a consolidated theory? *World Neurosurg*. 2016;85:8-9.

9. Kotan D, Aydin MD, Gundogdu C, Aygul R, Aydin N, Ulvi H. Parallel development of choroid plexus degeneration and meningeal inflammation in subarachnoid hemorrhage: experimental study. *Adv Clin Exp Med*. 2014;23:699-704.

10. Mashaly HA, Provencio JJ. Inflammation as a link between brain injury and heart damage: the model of subarachnoid hemorrhage. *Cleve Clin J Med*. 2008;75(suppl 2):S26-S30.

11. Gundersen HJ. Stereology of arbitrary particles. A review of unbiased number and size estimators and the presentation of some new ones, in memory of William R. Thompson. *J Microsc*. 1986;143:3-45.

12. Gundersen HJ, Bendtsen TF, Korbo L, Marcussen N, Møller A, Nielsen K, et al. Some new, simple and efficient stereological methods and their use in pathological research and diagnosis. *APMIS*. 1988;96:379-394.

13. Sterio DC. The unbiased estimation of number and sizes of arbitrary particles using the disector. *J Microsc*. 1984;134:127-136.

14. Yılmaz A, Aydın MD, Kanat A, Musluman AM, Atlas S, Aydın Y, et al. The effect of choroidal artery vasospasm on choroid plexus ınjury in subarachnoid haemorrhage: experimental study. *Turk Neurosurg*. 2011;21:477-482.

15. Niemelä M, Marbacher S. Acute hydrocephalus after subarachnoid hemorrhage—can it be caused by water vesicles of choroid plexuses? *World Neurosurg*. 2013;80:307-308.

16. Turkmenoglu ON, Kanat A, Yolas C, Aydin MD, Ezirmik N, Gundogdu C. First report of ımportant causal relationship between the Adamkiewicz artery vasospasm and dorsal root ganglion cell degeneration in spinal subarachnoid hemorrhage: an experimental study using a rabbit model. *Asian J Neurosurg*. http://dx.doi.org/10.4103/1793-5482.145572.

17. Aydin MD, Kanat A, Turkmenoglu ON, Yolas C, Gundogdu C, Aydın N. Changes in number of water-filled vesicles of choroid plexus in early and late phase of experimental rabbit subarachnoid hemorrhage model: the role of petrous ganglion of glossopharyngeal nerve. *Acta Neurochir (Wien)*. 2014;156:1311-1317.

18. Yolas C, Kanat A, Aydin MD, Ozturk C, Kabalar E, Akca N, et al. The important liaison between the Onuf's nucleus-pudendal nerve ganglia complex degeneration and urinary retention in spinal subarachnoid hemorrhage: an experimental study. *World Neurosurg*. 2016;89:208-214.

19. Meller ST, Dennis BJ. Quantitative Nissl study of the neuronal types, and recognition of cytoarchitectural subdivisions, within the rabbit periaqueductal gray. *J Comp Neurol*. 1990;302:87-99.

20. Aydin MD, Bayram E, Atalay C, Aydin N, Erdogan AR, Gundogdu C, et al. The role of neuron numbers of the petrosal ganglion in the determination of blood pressure: an experimental study. *Minim Invasive Neurosurg*. 2006;49:359-366.

21. Aydin MD, Kanat A, Yilmaz A, Cakir M, Emet M, Cakir Z, et al. The role of ischemic neurodegeneration of the nodose ganglia on cardiac arrest after subarachnoid hemorrhage: an experimental study. *Exp Neurol*. 2011;230:90-95.

22. Eseoglu M, Yilmaz I, Karalar M, Aydin MD, Kayaci S, Gundogdu C, et al. The role of sympathectomy on the regulation of basilar artery volume changes in steno-occlusive carotid artery modeling after bilateral common carotid artery ligation: an animal model. *Acta Neurochir (Wien)*. 2014;156:963-969.

23. Kanat A, Turkmenoglu O, Aydin MD, Yolas C, Aydin N, Gursan N, et al. Toward changing of the pathophysiologic basis of acute hydrocephalus after subarachnoid hemorrhage: a preliminary experimental study. *World Neurosurg*. 2013;80:390-395.

24. Kanat A. Pathophysiology of acute hydrocephalus after subarachnoid hemorrhage. *World Neurosurg*. 2014;82:e386-387.

25. Palade C, Ciurea AV, Nica DA, Savu R, Moisa HA. Interference of apoptosis in the pathophysiology of subarachnoid hemorrhage. *Asian J Neurosurg*. 2013;8:106-111.

26. Lackner P, Vahmjanin A, Hu Q, Krafft PR, Rolland W, Zhang JH. Chronic hydrocephalus after experimental subarachnoid hemorrhage. *PLoS One*. 2013;8:e6957.

27. Lindvall M, Edvinsson L, Owman C. Histochemical, ultra-structural, and functional evidence for a neurogenic control of CSF production from the choroid plexus. *Adv Neurol*. 1978;20:111-120.

28. Yolas C, Kanat A, Aydin MD, Turkmenoglu ON, Gundogdu C. Important casual association of carotid body and glossopharyngeal nerve and lung following experimental subarachnoid hemorrhage in rabbits. First report. *J Neurol Sci*. 2014;336:220-226.

29. Kanat A, Kayaci S, Yazar U, Sahin Y, Yaman O, Guvercin AR. One of the giants of neurological surgery left us more than a decade ago, and neurosurgical literature did not show much interest. *Neurol Neurochir Pol*. 2011;45:63-67.

30. Erixon HO, Sorteberg A, Sorteberg W, Eide PK. Predictors of shunt dependency after aneurysmal subarachnoid hemorrhage: results of a single-center clinical trial. *Acta Neurochir (Wien)*. 2014;156:2059-2069.

31. Kazdal H, Kanat A, Sen A, Kirbas S, Ardic G, Tufekci A, et al. A novel clinical observation in neuroleptic malignant-like syndrome: first demonstration of early progression of hydrocephalus. *J Clin Psychopharmacol*. 2015;35:211-212.

32. Ozturk C, Kanat A, Aydin MD, Yolas C, Kabalar ME, Gundogdu B, et al. The impact of L5 dorsal root ganglion degeneration and Adamkiewicz artery vasospasm on descending colon dilatation following spinal subarachnoid hemorrhage: an experimental study; first report. *J Craniovertebr Junction Spine*. 2015;6:69-75.

33. Kazdal H, Kanat A, Findik H, Sen A, Ozdemir B, Batcik OE, et al. Transorbital ultrasonographic measurement of optic nerve sheath diameter for intracranial midline shift in patients with head trauma. *World Neurosurg*. 2016;85:292-297.

34. Yolas C, Kanat A, Aydin MD, Altas E, Kanat IF, Kazdal H, et al. Unraveling of the effect of nodose ganglion degeneration on the coronary artery vasospasm after subarachnoid hemorrhage: an experimental study. *World Neurosurg*. 2016;86:79-87.

Conflict of interest statement: The authors declare that the article content was composed in the absence of any commercial or financial relationships that could be construed as a potential conflict of interest.

Received 1 February 2016; accepted 17 March 2016

Citation: World Neurosurg. (2016) 90:484-491.
http://dx.doi.org/10.1016/j.wneu.2016.03.049

Journal homepage: ***www.WORLDNEUROSURGERY.org***

Available online: ***www.sciencedirect.com***